Evidence of spin reorientation in $YbFe_6Ge_6$ from neutron diffraction and ^{57}Fe Mössbauer experiments

2000 J. Phys.: Condens. Matter 12 1085

(http://iopscience.iop.org/0953-8984/12/6/325)

J. Phys.: Condens. Matter **12** (2000) 1085–1095. Printed in the UK PII: S0953-8984(00)08111-X

Evidence of spin reorientation in $YbFe_6Ge_6$ from neutron diffraction and ^{57}Fe Mössbauer experiments

T Mazet† and B Malaman

Laboratoire de Chimie du Solide Minéral, Université Henri Poincaré—Nancy I, Associé au CNRS (UMR 7555), BP 239, 54506 Vandoeuvre les Nancy Cédex, France

E-mail: thomas.mazet@lcsm.u-nancy.fr

Received 24 September 1999, in final form 17 November 1999

Abstract. High-resolution neutron diffraction and ^{57}Fe Mössbauer experiments have been performed on powder samples of the ternary intermetallic $YbFe_6Ge_6$. This compound crystallizes with a hexagonal structure ($P6/mmm$) which can be described as an ordered state intermediate between the $HfFe_6Ge_6$- and YCo_6Ge_6-type structures, with cell parameters suggesting that the Yb ion is in (or close to) a trivalent state. At room temperature, the Fe-sublattice magnetic arrangement consists of an antiferromagnetic stacking along the *c*-axis of the ferromagnetic (001) Fe planes with the easy direction of magnetization along [001]. Below about 85 K a spin-reorientation process occurs; a fraction $\gamma(T)$ of the iron moments rotate abruptly from the *c*-axis to a given direction in or close to the basal plane. This phenomenon allows the observation of anisotropic contributions to the total hyperfine field at the Fe site. At 4.2 K, approximately 18% of the iron moments remain along the *c*-axis. No long-range magnetic order of the Yb sublattice is observed, at least above 1.5 K. We also report ^{57}Fe Mössbauer investigations of the $HfFe_6Ge_6$-type $LuFe_6Ge_6$ compound.

1. Introduction

The RFe_6Ge_6 compounds (R = Mg, Sc–Ti, Y–Nb, Hf, Gd–Lu and U) [1–15] are known to crystallize in a variety of closely related structures depending on both R size and sample preparation procedure. All these structures may be seen as resulting from a more or less ordered insertion of the R element within the Ge_8 holes of the CoSn-type FeGe ($P6/mmm$) host framework. The smallest R elements insert in an orderly fashion in half of the Fe–Ge–Fe slabs of the binary parent compound, leading to the $HfFe_6Ge_6$-type structure ($P6/mmm$). The largest R elements partially occupy each of these slabs. In the latter case, a long-range R atomic ordering leads to more complex crystal structures which were first analysed in terms of intergrowth of $HfFe_6Ge_6$ and $ScFe_6Ga_6$ blocks [3, 16]. In the opposite case, this yields disordered variants of the $HfFe_6Ge_6$ type such as the YCo_6Ge_6 type or derivatives intermediate between these two types.

The magnetic properties of the RFe_6Ge_6 compounds have been the subject of extensive investigations [3–5, 7–13, 15]. These compounds are characterized by an antiferromagnetic ordering of the Fe sublattice at temperatures ranging between 450 K and 510 K (except for UFe_6Ge_6, for which $T_N = 322$ K [4]), while the R sublattice orders magnetically at much lower temperature (between 30 K for R = Gd and 3 K for R = Er [7–10, 15]; probably at 230 K for R = U [4]). Whatever the crystal structure [8–13, 15], when the sole Fe sublattice

† Author to whom any correspondence should be addressed. Telephone: +33-1683-912167.

0953-8984/00/061085+11$30.00

is ordered, the magnetic structures always consist of an antiferromagnetic stacking $(+ - + -)$ along the c_h-axis of the hexagonal (sub)cell of ferromagnetic $(001)_h$ Fe planes, with the Fe moments pointing along the c_h-axis and ordered Fe moment values ranging between 1.5 μ_B and 2.2 μ_B. Consequently, there is zero molecular field on the R sites; this may explain the low ordering temperature of the R sublattice solely due to R–R interactions.

The previous studies have shown that the R-sublattice ordering temperature does not depend on the distribution of R atoms [7–10, 14, 15]. By contrast, the R magnetic arrangement strongly depends on this distribution as illustrated by the occasionally different results reported for the same R atom [7, 15]. This is further shown by the influence of the annealing temperature on the Tb magnetic arrangement in $TbFe_6Ge_6$, which is correlated with subtle changes in the Tb distribution within the FeGe host framework [9, 10]. On the other hand, an influence of the microstructure on the Ho magnetic behaviour has been shown for $HoFe_6Ge_6$ [14, 15]. In all cases (R = Gd–Er), except for one of the $TbFe_6Ge_6$ samples of reference [10], the R-sublattice magnetic ordering does not affect the easy direction of the antiferromagnetic $(+ - + -)$ Fe arrangement. According to reference [7] the Tm sublattice does not order in $TmFe_6Ge_6$.

For the $LuFe_6Ge_6$ and $YbFe_6Ge_6$ compounds, only room temperature Mössbauer data are available [7], while reported neutron diffraction results are restricted to $LuFe_6Ge_6$ above 122 K [11]. To obtain more complete information, we have undertaken a detailed investigation of the microscopic magnetic properties of $YbFe_6Ge_6$ by means of neutron diffraction and ^{57}Fe Mössbauer spectroscopy experiments. In this paper, we also report results from a ^{57}Fe Mössbauer study of $LuFe_6Ge_6$ at 300 K and 4.2 K.

2. Experimental details

The compounds were prepared from commercially available high-purity elements. Pellets of mixtures of the elements with composition $Yb_{1.2}Fe_6Ge_6$ (to allow for the inevitable loss of Yb) and $LuFe_6Ge_6$ were compacted using a steel die and introduced into silica tubes sealed under argon (400 mm Hg). Preliminary homogenization treatments were conducted for one week at 750 °C and 900 °C for $YbFe_6Ge_6$ and $LuFe_6Ge_6$, respectively. The samples were then ground, compacted again, annealed for three weeks at identical temperatures and finally quenched in water.

Preliminary x-ray analyses (Guinier Co Kα) from scanned patterns have shown the single-phase nature of our samples. In both cases, the diffraction lines can all be indexed using the $HfFe_6Ge_6$ settings. The $LuFe_6Ge_6$ sample is undoubtedly of $HfFe_6Ge_6$ type, while the observed intensities of the (*hkl with l odd*) lines of $YbFe_6Ge_6$ are weaker than those expected for this type of structure. This suggests that a partial $HfFe_6Ge_6$-type ordering of the YCo_6Ge_6 structure has taken place, as previously described for the $LuFe_6Ge_6$ sample of reference [11], where a fraction of the Ge(2e) and Yb atoms are shifted by $c/2$ from their ideal positions. The cell parameters were determined by least-squares refinements using high-purity silicon as an internal standard and were found to be close to those previously reported [3]; that is: $a = 5.098(2)$ Å/$c = 8.094(3)$ Å and $a = 5.097(1)$ Å/$c = 8.083(2)$ Å for $YbFe_6Ge_6$ and $LuFe_6Ge_6$, respectively. Such cell parameters suggest that the Yb ion is in (or close to) a trivalent state ($4f^{13}$, $J = 7/2$).

Neutron diffraction experiments were carried out on powder samples of $YbFe_6Ge_6$ at the Institut Laue–Langevin (ILL), Grenoble. Several spectra were recorded between 300 K and 2 K using the D1B ($\lambda = 2.520$ Å) two-axis diffractometer, while two patterns were recorded at 150 K and 1.5 K with the high-resolution D1A ($\lambda = 1.911$ Å) instrument. The analysis of the patterns was performed by Rietveld profile refinements using the software FULLPROF [17].

Several ^{57}Fe Mössbauer spectra were recorded between 4.2 K and 300 K in standard

transmission geometry using a constant-acceleration spectrometer with a 25 mCi ^{57}Co source in a rhodium matrix. The data were analysed with a least-squares fitting program assuming Lorentzian peaks and using the full hyperfine Hamiltonian [18]. Isomer shifts are given with respect to that of metallic iron at room temperature.

3. Results and interpretation

3.1. Neutron diffraction study of $YbFe_6Ge_6$

3.1.1. Crystal structure and magnetic structure above 85 K. The neutron diffraction pattern collected at 150 K with the D1A two-axis diffractometer is shown in figure 1. No superlattice lines are observed; all peaks can be indexed on the basis of an $HfFe_6Ge_6$-type cell but the intensities of the (*hkl with l odd*) lines are weaker than those expected for this model. This confirms the partly disordered crystal structure (figure 2), intermediate between the $HfFe_6Ge_6$- and YCo_6Ge_6-type ones, deduced from preliminary x-ray analyses where the Ge(2e) and Yb atoms are distributed on two different sites: Ge_1 $(0, 0, z)$/Ge_1' $(0, 0, z + 1/2)$ and Yb $(0, 0, 1/2)$/Yb′ $(0, 0, 0)$, respectively. During the refinement, the site occupancy ratios of Ge_1/Ge_1' and Yb/Yb′ were constrained to have the same value. The refinement

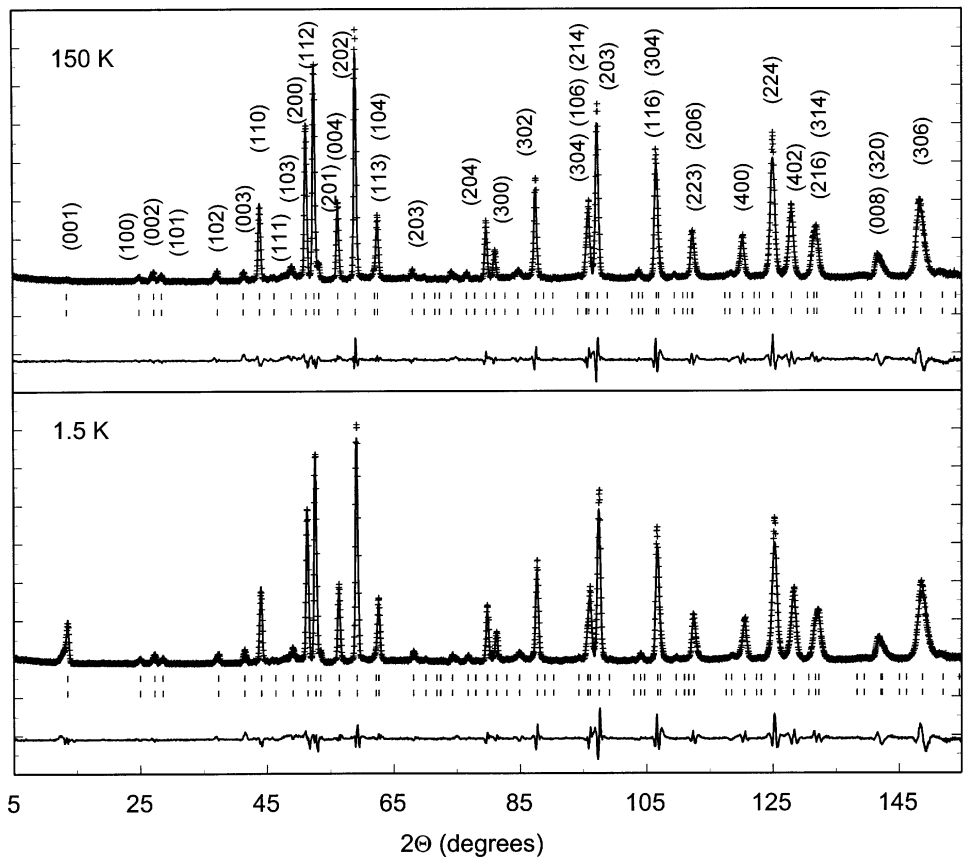

Figure 1. The neutron diffraction patterns of $YbFe_6Ge_6$ at 150 K and 1.5 K ($\lambda = 1.911$ Å).

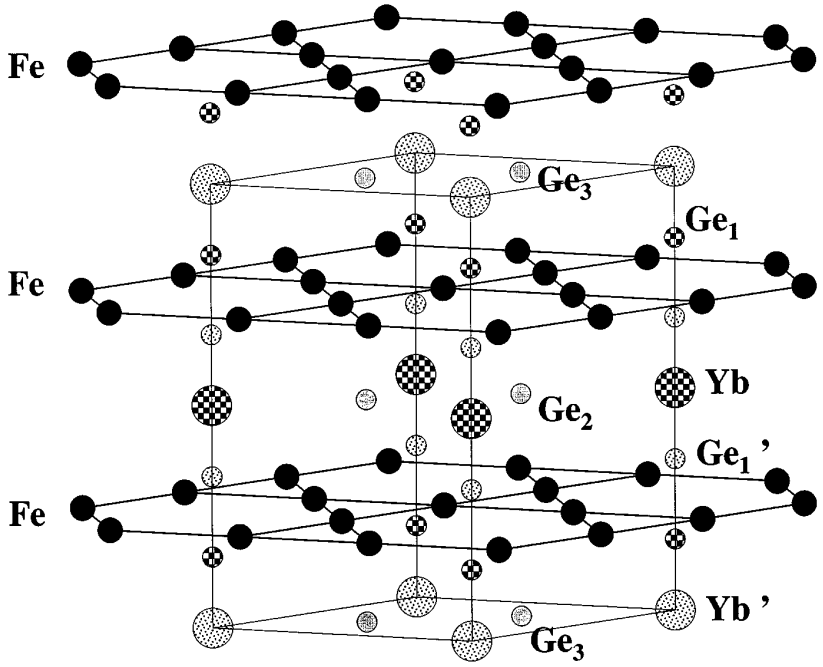

Figure 2. Crystal structure of $YbFe_6Ge_6$.

leads to a partial atomic disorder similar to that previously found in the $LuFe_6Ge_6$ sample of reference [11]. Furthermore, such observations are consistent with a magnetic structure built upon an antiferromagnetic stacking $(+ - + -)$ along the c-axis of the ferromagnetic easy-axis (001) Fe planes, as is always observed in the RFe_6Ge_6 intermetallics when the R sublattice is not magnetically ordered [8–13, 15]. At 150 K, the ordered Fe moment value refined to $\mu_{Fe} = 1.51(4)\ \mu_B$. The refined parameters and the residual factors are given in table 1.

Table 1. Refined parameters of $YbFe_6Ge_6$ ($P6/mmm$) derived from high-resolution neutron data at 150 K. $\mu_{Fe} = 1.51(4)\mu_B$, $a = 5.088(1)$ Å, $c = 8.085(1)$ Å, $R_{nucl} = 5.32\%$, $R_{mag} = 22.4\%$, $R_{wp} = 15.7\%$, $R_e = 5.83\%$.

Atom	Position	x	y	z	Occupancy	B_{iso} (Å^2)
Fe	(6i)	1/2	0	0.250(1)	1	0.11(3)
Ge_1	(2e)	0	0	0.153(1)	0.73(1)	0.28(6)
Ge_1'	(2e)	0	0	0.347(1)	0.27(1)	0.28(6)
Ge_2	(2c)	1/3	2/3	1/2	1	0.14(4)
Ge_3	(2d)	1/3	2/3	0	1	0.14(4)
Yb	(1b)	0	0	1/2	0.73(1)	0.42(7)
Yb′	(1a)	0	0	0	0.27(1)	0.42(7)

3.1.2. Neutron diffraction patterns below 85 K. Below about 85 K, the most important feature is a continuous and strong increase of the (001) line intensity whose nuclear contribution is weak (figure 1). The best fits were obtained considering a deviation from the c-axis of the antiferromagnetic direction of the Fe sublattice without any magnetic ordering of the Yb

sublattice. Assuming a single magnetic phase, refinement at 1.5 K shows that the easy direction makes an angle Φ of 56(3)° with the *c*-axis and $\mu_{Fe} = 1.72(5)\ \mu_B$ (table 2). Finally, we have to point out that the thermal dependence of the cell parameters reveals no anomalies.

Table 2. Refined parameters derived from high-resolution neutron data for $YbFe_6Ge_6$ at 1.5 K.

a (Å)	c (Å)	z_{Fe}	z_{Ge_1}	z'_{Ge_1}	μ_{Fe} (μ_B)	Φ (deg)	R_{nucl}, R_{mag}, R_{wp}, R_e (%)
5.082(1)	8.083(1)	0.250(1)	0.153(1)	0.347(1)	1.72(5)	56(3)	5.38, 13.7, 17.3, 5.30

3.2. ^{57}Fe Mössbauer spectroscopy

3.2.1. Preliminary remarks. In the hexagonal $YbFe_6Ge_6$ and $LuFe_6Ge_6$ compounds, the point symmetry at the (6i) iron site is $2mm$. Hence, as for the CoSn-type FeGe [20] and FeSn [18, 21] compounds, there are three sets of principal EFG axes for the three Fe atoms of an (001) Fe layer in a unit cell. They are along [110] [1$\bar{1}$0] [001], [100] [$\bar{1}\bar{2}$0] [001], [010] [210] [001] respectively (figure 3), although it is not possible to know *a priori* which is the principal Z-axis. For FeGe and FeSn it has been shown that the principal Z-axis lies in the basal plane. According to the point charge calculations of reference [5] this axis remains in the basal plane for the RFe_6Ge_6 series. Therefore, these systems may, like the well-known RFe_2 Laves phases [28–30] or like the Fe_3Sn_2 [25] and FeSn [19, 22] compounds, present several Zeeman patterns for crystallographically equivalent Fe atoms depending on the orientation of the magnetization direction with respect to the principal EFG axes.

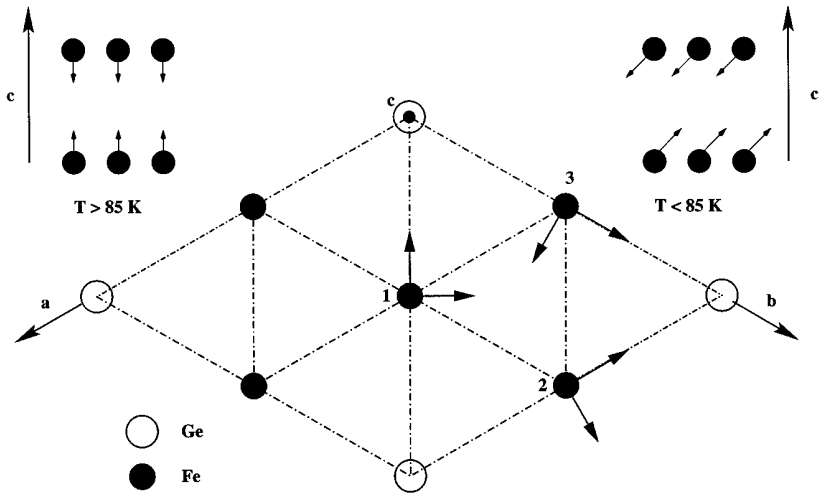

Figure 3. The three sets of principal axes of the EFG tensor for iron atoms in the basal plane of $YbFe_6Ge_6$, together with schematic representations of the Fe-sublattice magnetic arrangement above and below the spin-reorientation temperature ($T_{SR} \approx 85$ K).

3.2.2. $YbFe_6Ge_6$. Two types of spectrum are obtained in the magnetic state (figure 4). Above the spin-reorientation temperature ($T_{SR} \approx 85$ K) deduced from neutron diffraction experiments, only a classical single sextuplet is observed. Below 85 K, the spectra consist of six broad and asymmetric groups of lines which evolve with temperature.

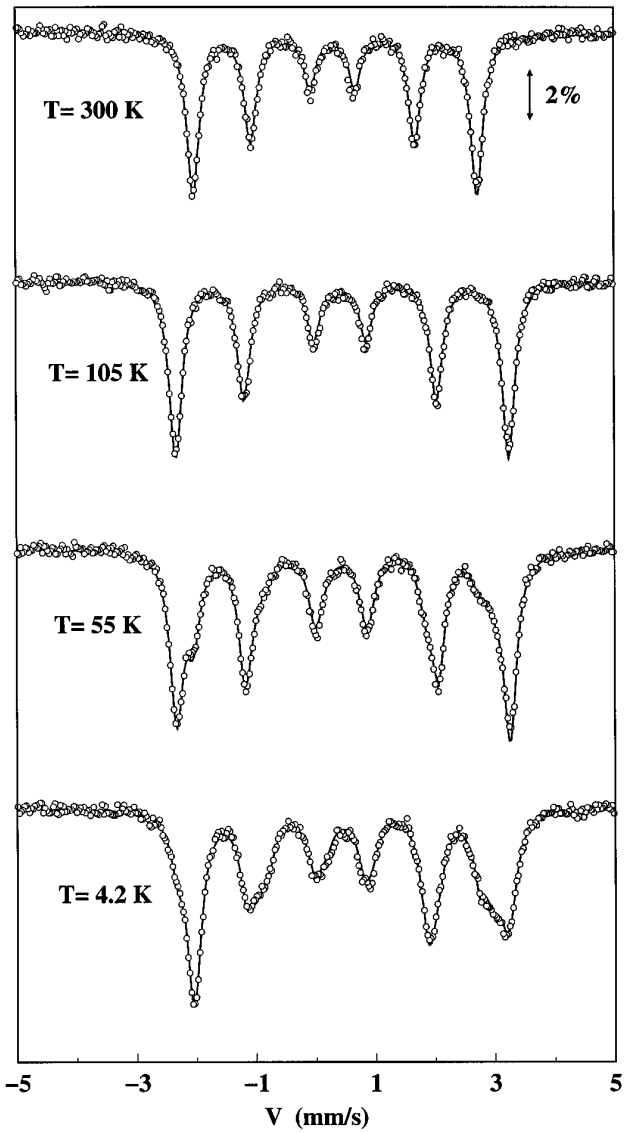

Figure 4. ^{57}Fe Mössbauer spectra of $YbFe_6Ge_6$ at several temperatures together with their least-squares envelopes.

In the magnetic state, the apparent quadrupolar splitting (2ϵ) is given to first order by

$$2\epsilon = \Delta\left[\frac{3\cos^2\theta - 1 + \eta\sin^2\theta\cos 2\phi}{2}\right] \tag{1}$$

where θ and ϕ are the polar and azimuthal angles of the hyperfine-field direction with respect to the EFG frame of reference, respectively, while the asymmetry parameter η ($0 \leqslant \eta \leqslant 1$) and $\Delta = eQV_{zz}/2$ have the usual definitions. When equation (1) holds, the relevant range of θ is seen to be $0^\circ \leqslant \theta \leqslant 90^\circ$. Despite the fact that the Z-axis could not be specified *a priori* from the point symmetry at the Fe site, it can nevertheless be concluded that θ is either 0° or 90°

when the direction of the Fe hyperfine field is along the c-axis. By contrast, if the latter lies in the basal plane, θ may either be 90° (Z-axis parallel to $\boldsymbol{c}$) or may *a priori* range between 0° and 90° for a given Fe site. Assuming that the quadrupole splitting Δ does not vary significantly at the magnetic transition, as usually observed:

$$\Delta_p = \Delta\sqrt{(1+\eta^2/3)} \tag{2}$$

where Δ_p is the total quadrupole splitting in the paramagnetic state. In reference [5], a $|\Delta_p|$ value of 0.27 mm s^{-1} was measured for the RFe_6Ge_6 series. Fits at several temperature between 300 K and 85 K show that 2ϵ is constant and has a mean value of 0.03 ± 0.01 mm s^{-1}, in good agreement with the room temperature result of reference [7]. The Fe moments are known to be parallel to the c-axis when $T > T_{SR}$. The angle θ is therefore either 0° or 90° while ϕ is irrelevant for $\theta = 0°$ (equation (1)) and equal either to 0° or to 90° for $\theta = 90°$. The only solution consistent both with $2\epsilon = 0.03$ mm s^{-1}, $|\Delta_p| = 0.27$ mm s^{-1} and with equations (1) and (2) is $\theta = 90°$: the principal Z-axis lies in the basal plane. Further, for $\theta = 90°$ a significant reduction of the angular factor of equation (1), which is necessary to account for the small value of 2ϵ, can only occur if η is close to 1 and if $\phi = 0°$. A supplementary consequence is that Δ_p and Δ are negative as also reported for FeGe [20], FeSn [19, 22] and Fe_3Sn_2 [25]. To summarize, the principal Y- and Z-axes of the EFG tensor lie in the basal plane while the principal X-axis is along $\boldsymbol{c}$. Our fittings at temperatures between 300 K and 85 K, carried out constraining the θ- and ϕ-angles to 90° and 0° respectively, yield $\Delta \approx -0.25$ mm s^{-1} and $\eta \approx 0.8$ (table 3). Large η-values were similarly reported for FeSn [19, 22].

Table 3. Hyperfine interaction parameters of $YbFe_6Ge_6$ above the spin-reorientation temperature ($T_{SR} \approx 85$ K).

T (K)	$\Gamma \pm 0.01$ (mm s^{-1})	IS ± 0.01 (mm s^{-1})	$\Delta \pm 0.03$ (mm s^{-1})	$\eta \pm 0.1$	$H \pm 0.1$ (T)
300	0.25	0.33	−0.26	0.7	14.8
240	0.26	0.37	−0.27	0.8	16.1
195	0.25	0.40	−0.25	0.8	16.7
150	0.28	0.42	−0.30	0.8	17.2
105	0.26	0.44	−0.26	0.8	17.3

Attempts to fit the 4.2 K Mössbauer spectrum with two or three hyperfine components were unsuccessful, resulting in very broad peaks in each sextet ($\Gamma \approx 0.36$ mm s^{-1}) and large χ^2-values. Satisfactory fits were obtained by considering four subspectra divided into two subgroups. In this last fitting procedure, we assume that only a fraction of the iron atoms have moments which rotate from the c-axis to a given direction to be specified. The isomer shifts, linewidths and values of Δ and η were therefore constrained to be respectively equal for the four subspectra (table 4) as expected from the crystallographic structure. Moreover, we were led to consider that one component has a hyperfine-field value similar to that found above the spin-reorientation temperature, with θ and ϕ fixed at values of 90° and 0°, respectively, as explained above (the first subgroup for the iron spins staying along the c-axis). We further considered three other components with equal intensity but different angular parameters and hyperfine-field values to be fitted independently (the second subgroup corresponding to iron spins not along the c-axis). To avoid introducing a ϕ-distribution, virtually impossible to deduce from such spectra, we also assumed that the iron spins of the second subgroup lie in the basal plane; hence the ϕ-angles of these components were constrained to 90°. The latter assumption, further discussed below, has only a limited effect on the fitted hyperfine parameter values. The results of our fittings at 4.2 K are given in table 4. Within fitting errors, our fitted θ-values are consistent with a unique magnetization direction in the basal plane and

Table 4. Hyperfine interaction parameters of $YbFe_6Ge_6$ at 4.2 K.

I (%)	$\Gamma \pm 0.01$ (mm s^{-1})	IS ± 0.01 (mm s^{-1})	$\Delta \pm 0.03$ (mm s^{-1})	$\eta \pm 0.1$	$\theta \pm 8$ (deg)	$H \pm 0.1$ (T)
27.4	0.27	0.46	−0.25	0.7	77	16.4
27.4	0.27	0.46	−0.25	0.7	56	15.5
27.4	0.27	0.46	−0.25	0.7	17	14.8
17.8	0.27	0.46	−0.25	0.7	90	17.4

not along the [100] or [210] directions. Further fits at intermediate temperatures confirmed our interpretation and showed only a variation in the relative intensity of the preceding subgroups without notable changes in the refined hyperfine parameter values as compared to those of the 4.2 K spectrum.

In summary, we have shown that below 85 K a fraction $\gamma(T)$ of the iron moments rotate abruptly from the c-axis to a given direction in or close to the basal plane, as already observed in Fe_3Sn_2 [25–27], although it is not possible to specify the precise orientation of these moments. The fraction $\gamma(T)$ increases when lowering the temperature, being about 82% at 4.2 K (table 4).

3.2.3. $LuFe_6Ge_6$. The ^{57}Fe Mössbauer spectra of $LuFe_6Ge_6$ recorded at 300 K and 4.2 K are shown in figure 5. They both consist of a single sextuplet and hence do not reveal any reorientation of the iron moments down to 4.2 K. The hyperfine parameters are close to those found for the Yb-based compound above 85 K (table 5). The hyperfine-field value is however slightly lower than it is for $YbFe_6Ge_6$ when the iron moments are parallel to the c-axis, in agreement with the room temperature results of reference [7]. It is worth noting that, as found

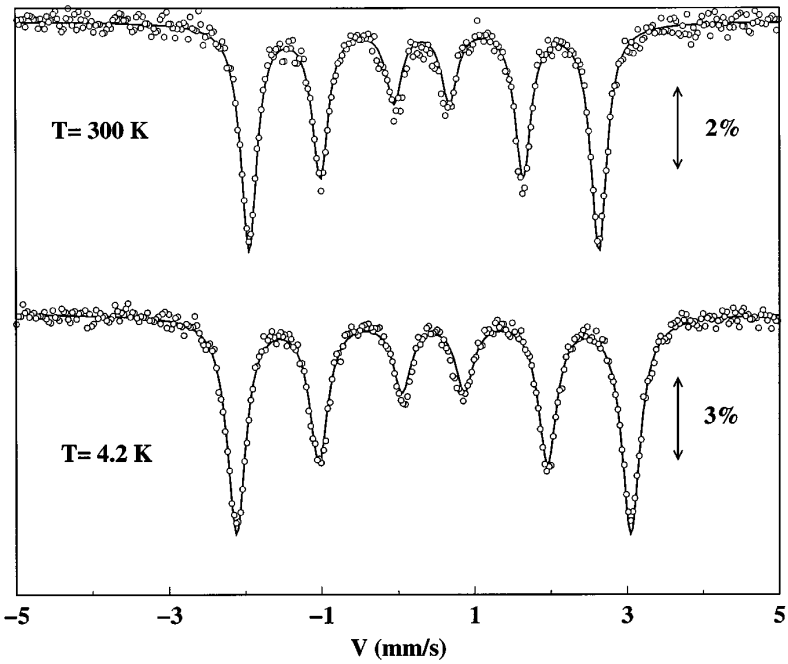

Figure 5. ^{57}Fe Mössbauer spectra of $LuFe_6Ge_6$ at 300 K and 4.2 K together with their least-squares envelopes.

Table 5. Hyperfine interaction parameters of $LuFe_6Ge_6$ at 300 K and 4.2 K.

T (K)	$\Gamma \pm 0.01$ (mm s^{-1})	IS ± 0.01 (mm s^{-1})	$2\epsilon \pm 0.01$ (mm s^{-1})	$H \pm 0.1$ (T)
300	0.25	0.33	0.03	14.3
4.2	0.30	0.46	0.00	16.1

for the binary FeGe parent compound [12, 20], a slight broadening of the lines is observed at low temperature. For the latter compound, characterized by the same easy-axis antiferromagnetic arrangement of the Fe moments at high temperature, neutron diffraction experiments on single crystal have shown that below 55 K the structure changes to a c-axis double cone with a cone half-angle of 14° at 4.2 K [31]. Similarly, in $LuFe_6Ge_6$, the possibility a small spread in the iron moment direction at low temperature cannot be excluded.

4. Discussion

From our neutron diffraction and ^{57}Fe Mössbauer experiments we have shown that in $YbFe_6Ge_6$ below about 85 K the moments of a fraction $\gamma(T)$ of the iron atoms rotate abruptly from the c-axis. Our ^{57}Fe Mössbauer results indicate that approximately 18% of the iron moments remain along the c-axis at 4.2 K. Hence the Φ-angle of 56(3)° between the c-axis and the easy direction of magnetization of the Fe sublattice that is deduced from the 1.5 K neutron refinement assuming a single magnetic phase is slightly underestimated. Therefore, assuming that 15% of the iron moments are along the c-axis at 1.5 K, the 'actual' Φ-angle would be 64(3)°. The latter angle disagrees with the basal-plane arrangement of the rotated spins assumed to fit the low-temperature ^{57}Fe Mössbauer spectra. However, it is worth noting that a similar problem occurs in the Fe_3Sn_2 compound ($R\bar{3}m$) [24], whose Fe–Sn basal planes are crystallographically similar to those of the present compound. The magnetic structure of Fe_3Sn_2 is also characterized by ferromagnetic (001) Fe planes and by a spin-reorientation process below 220 K. For the latter compound, powder neutron diffraction experiments give a Φ-angle of about 60° between the c-axis and the moment direction while both neutron diffraction with external fields and ^{119}Sn Mössbauer spectroscopy indicate an iron moment direction in the basal plane [25–27]. This discrepancy was accounted for by a modification of the conventional iron magnetic form factor due to the localization of the spin carriers along the [001] direction [26]. Although it is difficult to decide whether or not in $YbFe_6Ge_6$ the moments lie in the basal plane, both techniques allow the conclusion to be reached that the iron moments make an angle ranging typically between 25° and 0° with the basal plane.

The four iron sites used to fit the low-temperature Mössbauer spectra are characterized by four hyperfine-field values. Such field differences for a unique crystallographic site are due to the contribution of anisotropic hyperfine fields to the total field [21–23, 25, 28–30]. These anisotropic hyperfine fields make the total hyperfine-field direction deviate from that of the magnetization, and the component parallel to the magnetization can be expressed, in a first-order approximation, in the general form [23]

$$H = H_{iso} + H_a \left[\frac{3\cos^2\theta - 1 + \eta' \sin^2\theta \cos 2\phi}{2} \right] \tag{3}$$

where H_{iso} and H_a are respectively the isotropic and anisotropic contributions to the total hyperfine field $\boldsymbol{H}$ parallel to the magnetization direction, and η' is an asymmetry parameter related to the anisotropy of the hyperfine dipolar tensor. From band-structure calculations [32], it is now clearly established that the main contribution to the total hyperfine field at nuclei of

transition metal atoms (i.e. the Fermi contact interaction) is dominated by the polarization of the s core electrons. Because of the attractive nature of the exchange interaction this leads to a negative magnetization at the nucleus (i.e. a negative hyperfine field). We assume consistently that our experimental hyperfine-field values are negative. From relation (3) and our experimental data, we estimate that: $H_{iso} \approx -16$ T, $H_a \approx 2.5$ T and $\eta' \approx 0.3$. The anisotropic contribution was also found to be positive in Fe_3Sn_2 [25] and in $Fe_{1-x}Mn_xSn$ ($0 \leqslant x \leqslant 0.2$) solid solutions [23] with a similar magnitude. These anisotropic fields cannot be fully accounted for by the lattice dipolar fields and are probably due to contributions of the atom's own electrons (i.e. local dipolar and/or orbital fields).

The spin-reorientation process observed in $YbFe_6Ge_6$ is a unique phenomenon in the RFe_6Ge_6 series. For all RFe_6Ge_6 compounds, the $(+ - + -)$ antiferromagnetic arrangement of the Fe sublattice with moments pointing along the c_h-axis seemed to be a well-established rule, whatever the crystal structure, when the R sublattice is not magnetically ordered [8–13, 15], as observed for instance in the present ^{57}Fe Mössbauer study of $LuFe_6Ge_6$. Even when the R sublattice is magnetically ordered, a spin reorientation of the Fe sublattice was reported only for one $TbFe_6Ge_6$ sample in reference [15]. Assuming that the sample-independent R ordering temperature (30 K–3 K from Gd to Er [7–11, 15]) scales with the de Gennes factor, the Yb sublattice is not expected to order, in agreement with our neutron diffraction results. We conclude that in $YbFe_6Ge_6$, the spin-reorientation phenomenon can therefore no longer be associated with a long-range magnetic ordering of the Yb sublattice, considering moreover that the reorientation occurs below 85 K, but we have not yet been able to identify the mechanism responsible for the spin reorientation in this compound. However, the particular valence properties of the Yb ion [33] are undoubtedly involved. Finally, the unusual nature of the spin-reorientation process as inferred from our ^{57}Fe Mössbauer study might originate from a complex microstructure (microtwinning, stacking faults, ...) as found for $HoFe_6Ge_6$ [14].

5. Conclusions

We have shown by using both neutron diffraction and the ^{57}Fe Mössbauer effect that a spin-reorientation process occurs in $YbFe_6Ge_6$ below about 85 K. The moments of a fraction $\gamma(T)$ of the iron atoms rotate abruptly from the c-axis to a given direction close to or in the basal plane. At 4.2 K approximately 18% of these moments remain along the c-axis. This phenomenon cannot be associated with a magnetic ordering of the Yb sublattice and is therefore the first example within the RFe_6Ge_6 series where the easy direction of magnetization is not along the c_h-axis when the R sublattice is not magnetically ordered. Other experiments are needed to understand the origin of this spin reorientation.

Acknowledgments

We thank G Le Caër for enlightening discussions. We are also grateful to R Welter for his technical assistance during the low-temperature ^{57}Fe Mössbauer data acquisition. We are indebted to the Institut Laue–Langevin of Grenoble (France) for the provision of research facilities.

References

[1] Bucholz W and Schuster H U 1978 *Z. Naturf.* b **33** 877
[2] Olenitch R R, Aksel'rud L G and Yarmoliuk Ya P 1981 *Dopov. Akad. Nauk. Ukr. RSR* A **2** 84
[3] Venturini G, Welter R and Malaman B 1992 *J. Alloys Compounds* **185** 99

[4] Goncalves A P, Waerenborgh J C, Bonfait G, Amaro A, Godinho M M, Almeida M and Spirlet J C 1994 *J. Alloys Compounds* **204** 59
[5] Wang Y B, Wiarda D, Ryan D H and Cadogan J M 1994 *IEEE Trans. Magn.* **30** 4951
[6] Dzyanyi R B, Bodak O I, Aksel'rud L G and Pavlyuk V V 1995 *Inorg. Mater.* **31** 987
[7] Ryan D H and Cadogan J M 1996 *J. Appl. Phys.* **79** 6005
[8] Oleksyn O, Schobinger-Papamantellos P, Rodriguez-Carvajal J, Brück E and Buschow K H J 1997 *J. Alloys Compounds* **257** 36
[9] Schobinger-Papamantellos P, Oleksyn O, Rodriguez-Carvajal J, Brück A and Buschow K H J 1998 *J. Magn. Magn. Mater.* **182** 96
[10] Zaharko O, Schobinger-Papamantellos P, Ritter C, Rodriguez-Carvajal J and Buschow K H J 1998 *J. Magn. Magn. Mater.* **187** 293
[11] Schobinger-Papamantellos P, Buschow K H J, de Boer F R, Ritter C, Isnard O and Fauth P 1998 *J. Alloys Compounds* **267** 59
[12] Cadogan J M, Ryan D H, Swainson I P and Moze O 1998 *J. Phys.: Condens. Matter* **10** 5383
[13] Nishihara R, Akimitsu M, Hori T, Niida H, Ohoyama K, Ohashi M, Yamaguchi Y and Nagawa Y 1999 *J. Magn. Magn. Mater.* **196+197** 665
[14] Oleksyn O, Nissen H-U and Wessicken R 1998 *Phil. Mag. Lett.* **77** 275
[15] Zaharko O, Schobinger-Papamantellos P, Rodriguez-Carvajal J and Buschow K H J 1999 *J. Alloys Compounds* **288** 50
[16] Chafik El Idrissi B, Venturini G and Malaman B 1991 *Mater. Res. Bull.* **26** 1331
[17] Rodriguez-Carvajal J 1993 *Physica* B **192** 55
[18] Le Caër G, private communication
[19] Häggström L, Ericsson T, Wäppling R and Chandra K 1975 *Phys. Scr.* **11** 47
[20] Häggström L, Ericsson T, Wäppling R and Karlsson E 1975 *Phys. Scr.* **11** 55
[21] Kulshreshtha S K and Raj P 1980 *J. Phys. F: Met. Phys.* **10** 1841
[22] Kulshreshtha S K and Raj P 1981 *J. Phys. F: Met. Phys.* **11** 281
[23] Kulshreshtha S K and Raj P 1982 *J. Phys. F: Met. Phys.* **12** 377
[24] Malaman B, Roques B, Courtois A and Protas J 1976 *Acta Crystallogr.* B **32** 1348
[25] Le Caër G, Malaman B and Roques B 1978 *J. Phys. F: Met. Phys.* **8** 323
[26] Malaman B, Fruchart D and Le Caër G 1978 *J. Phys. F: Met. Phys.* **8** 2389
[27] Le Caër G, Malaman B, Häggström L and Ericsson T 1979 *J. Phys. F: Met. Phys.* **9** 1905
[28] Bowden G J, Bunbury D St P, Guimarães A P and Snyder R E 1968 *J. Phys. C: Solid State Phys.* **1** 1376
[29] Raj P and Kulshreshtha S K 1980 *J. Physique* **41** 1487
[30] Meyer C, Hartmann-Boutron F, Gros Y, Berthier Y and Buevoz J L 1981 *J. Physique* **42** 605
[31] Bernhard J, Lebech B and Beckman O 1984 *J. Phys. F: Met. Phys.* **14** 2379
[32] Akai H, Akai M, Blügel S, Drittler B, Ebert H, Terakura K, Zeller R and Dederichs P H 1990 *Prog. Theor. Phys. Suppl.* **101** 11
[33] Varma C M 1976 *Rev. Mod. Phys.* **48** 219